



**HAL**  
open science

# A DIRECT TIME PARALLEL SOLVER BY DIAGONALIZATION FOR THE WAVE EQUATION

Martin J Gander, Laurence Halpern, Johann J Rannou, Juliet J Ryan

► **To cite this version:**

Martin J Gander, Laurence Halpern, Johann J Rannou, Juliet J Ryan. A DIRECT TIME PARALLEL SOLVER BY DIAGONALIZATION FOR THE WAVE EQUATION. 2017. hal-01590347v1

**HAL Id: hal-01590347**

**<https://hal.science/hal-01590347v1>**

Preprint submitted on 19 Sep 2017 (v1), last revised 31 Dec 2018 (v2)

**HAL** is a multi-disciplinary open access archive for the deposit and dissemination of scientific research documents, whether they are published or not. The documents may come from teaching and research institutions in France or abroad, or from public or private research centers.

L'archive ouverte pluridisciplinaire **HAL**, est destinée au dépôt et à la diffusion de documents scientifiques de niveau recherche, publiés ou non, émanant des établissements d'enseignement et de recherche français ou étrangers, des laboratoires publics ou privés.

# A DIRECT TIME PARALLEL SOLVER BY DIAGONALIZATION FOR THE WAVE EQUATION

MARTIN J. GANDER\*, LAURENCE HALPERN†, JOHANN RANNOU‡, AND JULIET  
RYAN §

**Abstract.** With the advent of very large scale parallel computers, it has become more and more important to also use the time direction for parallelization when solving evolution problems. While there are many successful algorithms for diffusive problems, it has turned out to be substantially more difficult to solve hyperbolic problems in a time parallel fashion. We present here a mathematical analysis of a new method based on the diagonalization of the time stepping matrix proposed by Maday and Rønquist in 2007. Like for many time parallelization methods, this seems at first not to be a very promising approach, since this matrix is essentially triangular, and for a fixed time step even a Jordan block, and thus not diagonalizable. If one chooses however different time steps, diagonalization is possible, and one has to trade off between the accuracy due to necessarily having different time steps, and numerical errors in the diagonalization process of these almost non-diagonalizable matrices. We study this trade-off mathematically for the wave equation with a Crank-Nicolson discretization, and propose an optimization strategy for the choice of the parameters. We illustrate our results with numerical experiments for model wave equations in various dimensions, and also an industrial test case for the elasticity equations.

**1. Introduction.** Using the time direction in evolution problems for parallelization is an active field of research, for an overview, see [?]. Most of the methods developed for this purpose are iterative, see for example the parareal algorithm [?], whose convergence was analyzed in [?] for linear problems, where also convergence difficulties in the hyperbolic case were identified; for an analysis in the non-linear case, see [?]. A variation of the parareal algorithm using spectral deferred correction [?] led then to the PFASST algorithm [?], which is a multilevel method. Space-time multigrid methods were also developed, see [?] and references therein, and a new such method using only standard components can be found in [?] with excellent strong and weak scaling properties for parabolic problems. There is also the non-invasive MGRIT algorithm [?, ?], and it was shown in [?] that MGRIT is equivalent to an overlapping parareal algorithm, which led to a detailed non-linear convergence analysis for MGRIT [?]. Early versions of these space-time multigrid methods were based on waveform relaxation [?, ?], and there are also very successful Schwarz waveform relaxation methods for the time parallel solution of evolution partial differential equations [?, ?, ?, ?, ?], and the more recent Dirichlet-Neumann and Neumann-Neumann waveform relaxation methods [?, ?, ?]. These are among the very few space-time iterative methods that are effective for hyperbolic problems, see [?, ?, ?], since they use the finite speed of propagation for good space-time decompositions, and also the related tent-pitching approach [?] which removes the need for iteration completely by following in the decomposition the characteristics. A different approach for hyperbolic problems are the Krylov parareal methods [?, ?, ?, ?], which however have an important overhead due to orthogonalization.

As an alternative, one can use direct space-time parallel solvers, like RIDC [?],

---

\*Section de mathématiques, Université de Genève, 2-4 rue du Lièvre, CP 64, CH-1211 Genève 4, Switzerland. [Martin.Gander@unige.ch](mailto:Martin.Gander@unige.ch)

†LAGA, Université Paris XIII, 99 Avenue J.-B. Clément, 93430 Villetaneuse, France. [halpern@math.univ-paris13.fr](mailto:halpern@math.univ-paris13.fr)

‡ONERA, BP 72, 29 avenue de la Division Leclerc, 92322 Chatillon cedex, FRANCE, [johann.rannou@onera.fr](mailto:johann.rannou@onera.fr)

§ONERA, Chemin de la Hunière - BP 80100, 91123 Palaiseau cedex, FRANCE, [ryan@onera.fr](mailto:ryan@onera.fr)

which is ideal for multicore architectures and generates high order solutions in time in parallel at the runtime cost of an Euler time stepper. For linear hyperbolic problems, there is also the ParaExp algorithm [?] which is based on a fully overlapping decomposition and Krylov techniques. A further direct approach based on the diagonalization of the time stepping matrix was introduced in [?]; for a mathematical analysis of this approach for the heat equation, see [?].

We present and analyze a new such direct time parallel method based on diagonalization for hyperbolic problems. We consider as our model partial differential equation (PDE) the wave equation,

$$(1.1) \quad \begin{aligned} \partial_{tt}u - \Delta u &= 0 && \text{in } \Omega \times (0, T), \\ u &= 0 && \text{on } \partial\Omega, \\ (u, \partial_t u)(\cdot, 0) &= (f, g) && \text{in } \Omega. \end{aligned}$$

A popular implicit time integrator for the wave equation (??) is the Newmark scheme [?]: let  $\Delta_h$  be a space discretization of the Laplacian  $\Delta$ , and we thus want to discretize  $\ddot{u}_h - \Delta_h u_h = 0$  in time, where  $\ddot{u}_h := \partial_{tt}u_h$ . In the Newmark scheme, the additional unknown  $\dot{u}_h := \partial_t u_h$  is introduced, and one then approximates both  $u_h$  and  $\dot{u}_h$  on the time partition  $0 = t_0 < t_1 < t_2 < \dots < t_N = T$ ,  $k_n := t_n - t_{n-1}$ , by a time stepping rule involving the two parameters  $\beta$  and  $\gamma$ ,

$$(1.2) \quad \begin{aligned} u_h^{n+1} &= u_h^n + k_{n+1}\dot{u}_h^n + k_{n+1}^2((\frac{1}{2} - \beta)\ddot{u}_h^n + \beta\ddot{u}_h^{n+1}), \\ \dot{u}_h^{n+1} &= \dot{u}_h^n + k_{n+1}((1 - \gamma)\ddot{u}_h^n + \gamma\ddot{u}_h^{n+1}), \\ \ddot{u}_h^n - \Delta_h u_h^n &= 0, \end{aligned}$$

with given initial data  $u_h^0$  and  $\dot{u}_h^0$ .

Let  $I_t$  be the  $N \times N$  identity matrix associated with the time domain and  $I_x$  be the  $J \times J$  identity matrix associated with the spatial domain. Setting  $\mathbf{u} := (u_h^1, \dots, u_h^N)$ , and similarly for  $\dot{\mathbf{u}}$  and  $\ddot{\mathbf{u}}$ , and defining the matrices

$$\begin{aligned} B_1 &= \begin{pmatrix} \frac{1}{k_1} & & & \\ -\frac{1}{k_2} & \frac{1}{k_2} & & \\ 0 & \ddots & \ddots & \\ & & -\frac{1}{k_N} & \frac{1}{k_N} \end{pmatrix}, & B_2 &= \begin{pmatrix} 0 & & & \\ 1 & 0 & & \\ 0 & \ddots & \ddots & \\ & & 1 & 0 \end{pmatrix}, \\ C_1 &= \begin{pmatrix} \beta k_1 & & & \\ (\frac{1}{2} - \beta)k_2 & \beta k_2 & & \\ 0 & \ddots & \ddots & \\ & & (\frac{1}{2} - \beta)k_N & \beta k_N \end{pmatrix}, & C &= \begin{pmatrix} \gamma & & & \\ (1 - \gamma) & \gamma & & \\ 0 & \ddots & \ddots & \\ & & (1 - \gamma) & \gamma \end{pmatrix}, \end{aligned}$$

the scheme (??) can be written in the compact form

$$(1.3) \quad \begin{aligned} (B_1 \otimes I_x)\mathbf{u} &= (B_2 \otimes I_x)\dot{\mathbf{u}} + (C_1 \otimes I_x)\ddot{\mathbf{u}} + F, \\ (B_1 \otimes I_x)\dot{\mathbf{u}} &= (C \otimes I_x)\ddot{\mathbf{u}} + G, \\ \ddot{\mathbf{u}} - (I_t \otimes \Delta_h)\mathbf{u} &= 0, \end{aligned}$$

with the right hand sides

$$F = (\frac{1}{k_1}u_h^0 + \dot{u}_h^0 + (\frac{1}{2} - \beta)k_1\Delta_h u_h^0, 0, \dots, 0), \quad G = (\frac{1}{k_1}\dot{u}_h^0 + (1 - \gamma)\Delta_h u_h^0, 0, \dots, 0).$$

Solving the second equation in (??) for  $\dot{\mathbf{u}}$  using that for the Kronecker product  $(B_1 \otimes I_x)(B_2 \otimes I_x) = (B_1 B_2 \otimes I_x)$ , we get  $\dot{\mathbf{u}} = (B_1^{-1} \otimes I_x)((C \otimes I_x)\ddot{\mathbf{u}} + G)$ , which we insert into the first equation to obtain

$$(B_1 \otimes I_x)\mathbf{u} = ((B_2 B_1^{-1} C + C_1) \otimes I_x)\ddot{\mathbf{u}} + (B_2 B_1^{-1} \otimes I_x)G + F.$$

The matrix  $B_3 := B_2 B_1^{-1} C + C_1$  is a lower triangular matrix whose diagonal is that of  $C_1$ . Hence  $B_3$  is invertible, and we can solve for  $\ddot{\mathbf{u}}$  to obtain

$$\ddot{\mathbf{u}} = (B_3^{-1} \otimes I_x)\left((B_1 \otimes I_x)\mathbf{u} - (B_2 B_1^{-1} \otimes I_x)G - F\right).$$

Inserting this into the last equation in (??), we find

$$(1.4) \quad (B \otimes I_x - I_t \otimes \Delta_h)\mathbf{u} = \mathbf{f},$$

with

$$(1.5) \quad B = B_3^{-1} B_1, \quad \mathbf{f} = (B_3^{-1} \otimes I_x)((B_2 B_1^{-1} \otimes I_x)G + F).$$

Equation (??), is the matrix tensor-product form of the Newmark scheme for the wave equation in mixed form. It is equivalent to (??), and since the matrices are well-conditioned, it gives numerically the same solution. The velocity vector can be recovered using the equation

$$\dot{\mathbf{u}} = (B_1^{-1} \otimes I_x)((C \otimes \Delta_h)\mathbf{u} + G).$$

The key idea to solve a space-time problem written in tensor-product form (??) in a time parallel fashion from [?] is to diagonalize  $B$ . Since all matrices are lower triangular,  $B$  is lower triangular, and the diagonal of  $B$  equals  $(\frac{1}{\beta k_1^2}, \dots, \frac{1}{\beta k_N^2})$ . If all the time steps are different, then  $B$  is indeed diagonalizable,  $B = SDS^{-1}$ , where the diagonal matrix  $D$  contains the eigenvalues  $\frac{1}{\beta k_n^2}$  on the diagonal, and (??) can be written as

$$(1.6) \quad (S \otimes I_x)(D \otimes I_x - I_t \otimes \Delta_h)(S^{-1} \otimes I_x)\mathbf{u} = \mathbf{f}.$$

One can then solve (??) parallel in time performing the following 3 steps:

$$(1.7) \quad \begin{aligned} (a) \quad & \mathbf{g} = (S^{-1} \otimes I_x)\mathbf{f}, \\ (b) \quad & (\frac{1}{\beta k_n^2} - \Delta_h)\mathbf{w}^n = \mathbf{g}^n, \quad 1 \leq n \leq N, \\ (c) \quad & \mathbf{u} = (S \otimes I_x)\mathbf{w}. \end{aligned}$$

The main work, namely the  $N$  linear systems in space in step (b), can all be solved in parallel. We call this approach time parallelization by diagonalization. It was first introduced and analyzed numerically for wave propagation in [?, ?], motivated by the original invention in [?, ?] for diffusive problems the authors called tensor-product space-time solvers. We will analyze here specifically the Crank-Nicolson scheme, which corresponds to  $\beta = \frac{1}{4}$  and  $\gamma = \frac{1}{2}$  in the Newmark scheme (??). To see in what sense this corresponds to Crank-Nicolson, we first replace the last equation in (??) into the first two for these values of the parameters,

$$\begin{aligned} u_h^{n+1} &= u_h^n + k_{n+1} \dot{u}_h^n + \frac{k_{n+1}^2}{4} (\Delta_h u_h^n + \Delta_h u_h^{n+1}), \\ \dot{u}_h^{n+1} &= \dot{u}_h^n + \frac{k_{n+1}}{2} (\Delta_h u_h^n + \Delta_h u_h^{n+1}). \end{aligned}$$

Now from the second equation, we have  $\frac{1}{4}(\Delta_h u_h^n + \Delta_h u_h^{n+1}) = (\dot{u}_h^{n+1} - \dot{u}_h^n)/(2k_{n+1})$ , which when inserted into the right hand side of the first equation gives

$$(1.8) \quad \begin{aligned} u_h^{n+1} &= u_h^n + \frac{k_{n+1}}{2}(\dot{u}_h^n + \dot{u}_h^{n+1}), \\ \dot{u}_h^{n+1} &= \dot{u}_h^n + \frac{k_{n+1}}{2}(\Delta_h u_h^n + \Delta_h u_h^{n+1}), \end{aligned}$$

which is clearly Crank-Nicolson applied to the mixed formulation of the wave equation, which with  $v_h := \dot{u}_h$  is given by

$$\begin{aligned} \dot{u}_h &= v_h \\ \dot{v}_h &= \Delta_h u_h. \end{aligned}$$

Crank-Nicolson is second order accurate in time, and unconditionally stable. With a similar computation as for the Newmark scheme, we also obtain the tensor-product form (??) for the Crank-Nicolson scheme with

$$(1.9) \quad B = (C^{-1}B_1)^2, \quad \mathbf{f} = (C^{-1} \otimes I_x)((B_1C^{-1} \otimes I_x)F + G),$$

$\beta = \frac{1}{4}$ ,  $\gamma = \frac{1}{2}$ , and the same  $G$ , but with  $F = (\frac{1}{k_1}u_h^0 + \frac{1}{2}\dot{u}_h^0, 0, \dots, 0)$ .

**2. Analysis of time parallelization by diagonalization.** Using the time parallel solver (??) based on diagonalization requires some care: first, the time stepping matrix  $B$  is only diagonalizable if the time steps are all different, and this can lead to a larger discretization error compared to using equidistant time steps. Second, the condition number of the eigenvector matrix  $S$  increases exponentially with the number of time steps  $N$  to be done in parallel, which leads to inaccurate results in steps (a) and (c) of (??) because of roundoff error. One therefore needs to carefully and accurately estimate these two errors, to determine how many time steps can indeed be performed in parallel using (??) without losing accuracy.

In order to obtain such estimates in the wave equation case, we use a Fourier transform in space with Fourier variable  $\xi$ , and obtain  $\frac{\partial^2 \hat{u}}{\partial t^2} + |\xi|^2 \hat{u} = 0$ , which indicates that we need to study for fixed  $T$  and  $a > 0$  the algorithm (??) applied to the ordinary differential equation (ODE)

$$(2.1) \quad \ddot{u} + a^2 u = 0, \quad t \in (0, T),$$

with initial conditions  $u(0) = f$  and  $\dot{u}(0) = g$ . The Crank-Nicolson scheme for (??) is

$$(2.2) \quad \begin{aligned} u^n &= u^{n-1} + \frac{1}{2}k_n(\dot{u}^n + \dot{u}^{n-1}), \\ \dot{u}^n &= \dot{u}^{n-1} - \frac{a^2}{2}k_n(u^n + u^{n-1}), \end{aligned}$$

with initial conditions  $u^0 = f$  and  $\dot{u}^0 = g$ . Let  $U := (u, \frac{1}{a}\dot{u})$  be the solution of (??) including the derivative term which will be important for our estimates, and  $U^n := (u^n, \frac{1}{a}\dot{u}^n)$  be the discrete approximation defined by (??). We can then rewrite the continuous and discretized problems as

$$(2.3) \quad d_t U + aJU = 0, \quad (I + \frac{ak_n}{2}J)U^n = (I - \frac{ak_n}{2}J)U^{n-1}, \quad J := \begin{pmatrix} 0 & -1 \\ 1 & 0 \end{pmatrix},$$

with initial condition  $U(0) = U^0 = (f, \frac{g}{a})$ . For a given  $N$ , we now consider time steps given by a geometric partition  $\mathcal{T}_q := (k_1, \dots, k_N)$ ,  $k_n(q) := q^{n-1}k_1$  as it was

suggested in [?]. The constraint  $\sum_{n=1}^N k_n = T$  determines uniquely the value of the geometric time steps,

$$(2.4) \quad k_n = \frac{q^n}{\sum_{j=1}^N q^j} T.$$

We call  $U^n(\mathcal{T}_q)$  the corresponding sequence of solutions. The equidistant timestep  $\tilde{k} = \frac{T}{N}$  is obtained for  $q = 1$ .

**2.1. Estimation of the error due to the geometric time stepping.** We now present an accurate estimate for the increase in the truncation error caused by using a geometric time stepping with  $q = 1 + \varepsilon$ , compared to using equal time stepping, by studying the distance between  $U^N(\mathcal{T}_q)$  and  $U^N(\mathcal{T}_1)$ .

**THEOREM 2.1** (Asymptotic truncation error estimate). *For fixed  $a$ ,  $T$  and  $N$ , we obtain for  $\varepsilon$  small the error estimate*

$$(2.5) \quad \|U^N(\mathcal{T}_{1+\varepsilon}) - U^N(\mathcal{T}_1)\| = \phi\left(\frac{aT}{2N}, N\right)\varepsilon^2\|U^0\| + \mathcal{O}(\varepsilon^3),$$

where  $\phi(y, N) := \frac{N(N^2-1)}{6} \frac{y^3}{(1+y^2)^2}$ .

*Proof.* We first diagonalize the two systems (??) in the complex plane: let

$$P := \begin{pmatrix} 1 & 1 \\ i & -i \end{pmatrix}, \quad D := \begin{pmatrix} -1 & 0 \\ 0 & 1 \end{pmatrix},$$

which implies that  $P^{-1}JP = iD$  and  $P^{-1}(I - \alpha J)P = I - i\alpha D$ . Defining

$$\mu(t) := e^{-iat}, \quad \lambda_n := \frac{1 - i\frac{ak_n}{2}}{1 + i\frac{ak_n}{2}}, \quad \text{and} \quad \mu_n := \prod_{p=1}^n \lambda_p,$$

we obtain the diagonalized continuous and discrete solutions

$$U(t) = P \begin{pmatrix} \bar{\mu}(t) & 0 \\ 0 & \mu(t) \end{pmatrix} P^{-1}U_0, \quad U^n = P \begin{pmatrix} \bar{\mu}_n & 0 \\ 0 & \mu_n \end{pmatrix} P^{-1}U^0.$$

For a given  $N$ , we now estimate the change induced by the non equidistant time steps. For any partition  $\mathcal{T} = (k_1, \dots, k_N)$  of the interval  $(0, T)$ , we compare the solution  $U^N(\mathcal{T})$  to the solution  $U^N(\tilde{\mathcal{T}})$  obtained by the equidistant mesh  $\tilde{\mathcal{T}} = (\tilde{k}, \dots, \tilde{k})$  with  $\tilde{k} = T/N$ . Defining

$$\mu(\mathcal{T}) := \prod_{n=1}^N \frac{1 - i\frac{ak_n}{2}}{1 + i\frac{ak_n}{2}},$$

we find that

$$(2.6) \quad U^N(\mathcal{T}) - U^N(\tilde{\mathcal{T}}) = P \begin{pmatrix} \overline{\mu(\mathcal{T}) - \mu(\tilde{\mathcal{T}})} & 0 \\ 0 & \mu(\mathcal{T}) - \mu(\tilde{\mathcal{T}}) \end{pmatrix} P^{-1}U^0.$$

Taking norms, and noting that  $\|PV\|^2 = 2\|V\|^2$  and  $\|P^{-1}V\|^2 = \frac{1}{2}\|V\|^2$ , we get

$$(2.7) \quad \begin{aligned} \|U^N(\mathcal{T}) - U^N(\tilde{\mathcal{T}})\| &= |\mu(\mathcal{T}) - \mu(\tilde{\mathcal{T}})|\|U^0\|, \\ \|U^N(\tilde{\mathcal{T}}) - U(T)\| &= |\mu(\tilde{\mathcal{T}}) - e^{-iaT}|\|U^0\|. \end{aligned}$$

The second formula is the truncation error at the end of the time interval for equidistant timesteps. We next need to estimate the error in  $\mu$ , for which we use the following

LEMMA 2.2. *For fixed  $a, T$  and  $N$ , we have*

$$(2.8) \quad |\mu(\mathcal{T}) - \mu(\tilde{\mathcal{T}})| = \frac{a^3 \tilde{k}}{4(1 + \frac{a^2 \tilde{k}^2}{4})^2} \|\mathcal{T} - \tilde{\mathcal{T}}\|^2 + \mathcal{O}(\|\mathcal{T} - \tilde{\mathcal{T}}\|^3).$$

*Proof.* We write  $\mu(\mathcal{T})$  as

$$\mu(\mathcal{T}) = \prod_{n=1}^N \lambda(k_n), \quad \lambda(k) = \frac{1 - i\frac{ak}{2}}{1 + i\frac{ak}{2}}.$$

By the second order Taylor-Young formula, we have

$$\mu(\mathcal{T}) = \mu(\tilde{\mathcal{T}}) + \mu'(\tilde{\mathcal{T}}) \cdot (\mathcal{T} - \tilde{\mathcal{T}}) + \frac{1}{2} \mu''(\tilde{\mathcal{T}}) \cdot (\mathcal{T} - \tilde{\mathcal{T}}) \cdot (\mathcal{T} - \tilde{\mathcal{T}}) + \mathcal{O}(\|\mathcal{T} - \tilde{\mathcal{T}}\|^3).$$

We now compute the derivative,

$$(2.9) \quad \frac{\partial \mu}{\partial k_n}(\tilde{\mathcal{T}}) = \mu(\tilde{\mathcal{T}}) \frac{\lambda'(k_n)}{\lambda(k_n)} = \mu(\tilde{\mathcal{T}}) \frac{-ia}{1 + \frac{a^2 \tilde{k}^2}{4}},$$

and therefore obtain for the linear term

$$\mu'(\tilde{\mathcal{T}}) \cdot (\mathcal{T} - \tilde{\mathcal{T}}) = \mu(\tilde{\mathcal{T}}) \frac{-ia}{1 + \frac{a^2 \tilde{k}^2}{4}} \sum_n (k_n - \tilde{k}) = 0.$$

For the quadratic term, we differentiate (??) again with respect to  $k_n$ ,

$$(2.10) \quad \frac{\partial^2 \mu}{\partial k_n^2}(\tilde{\mathcal{T}}) = \mu(\tilde{\mathcal{T}}) a^2 \frac{-1 + i\frac{a\tilde{k}}{2}}{(1 + \frac{a^2 \tilde{k}^2}{4})^2}, \quad \frac{\partial^2 \mu}{\partial k_n \partial k_j}(\tilde{\mathcal{T}}) = \mu(\tilde{\mathcal{T}}) a^2 \frac{-1}{(1 + \frac{a^2 \tilde{k}^2}{4})^2},$$

and therefore obtain

$$\mu''(\tilde{\mathcal{T}}) \cdot (\mathcal{T} - \tilde{\mathcal{T}}) \cdot (\mathcal{T} - \tilde{\mathcal{T}}) = -a^2 \mu(\tilde{\mathcal{T}}) \frac{\sum_{n,j} (k_n - \tilde{k})(k_j - \tilde{k}) - i\frac{a\tilde{k}}{2} \sum_n (k_n - \tilde{k})^2}{(1 + \frac{a^2 \tilde{k}^2}{4})^2},$$

which gives

$$\mu(\mathcal{T}) = \mu(\tilde{\mathcal{T}}) - \frac{a^2 \mu(\tilde{\mathcal{T}})}{2} \frac{\sum_{n,j} (k_n - \tilde{k})(k_j - \tilde{k}) - i\frac{a\tilde{k}}{2} \sum_n (k_n - \tilde{k})^2}{(1 + \frac{a^2 \tilde{k}^2}{4})^2} + \mathcal{O}(\|\mathcal{T} - \tilde{\mathcal{T}}\|^3).$$

The first sum in the numerator is zero, and hence

$$\mu(\mathcal{T}) - \mu(\tilde{\mathcal{T}}) = \frac{i\mu(\tilde{\mathcal{T}}) a^3 \tilde{k} \sum_n (k_n - \tilde{k})^2}{4(1 + \frac{a^2 \tilde{k}^2}{4})^2} + \mathcal{O}(\|\mathcal{T} - \tilde{\mathcal{T}}\|^3),$$

which gives (??) when taking the modulus, since the quadratic term is purely imaginary and  $|\mu(\tilde{\mathcal{T}})| = 1$ .  $\square$

It remains to estimate  $\|\mathcal{T} - \tilde{\mathcal{T}}\|^2$ , which is done in

LEMMA 2.3. *The difference between the geometric and equal time partition satisfies the estimate*

$$(2.11) \quad \|\mathcal{T} - \tilde{\mathcal{T}}\|^2 = \sum_{n=1}^N (k_n - \tilde{k})^2 = \tilde{k}^2 \frac{N(N^2 - 1)}{12} \varepsilon^2 + \mathcal{O}(\varepsilon^3).$$

*Proof.* The time step  $k_n$  in (??) has for  $\varepsilon$  small the expansion  $k_n = \tilde{k}(1 + \alpha_n \varepsilon + \beta_n \varepsilon^2 + o(\varepsilon^2))$ , with  $\alpha_n = n - \frac{N+1}{2}$  and  $\beta_n = n(n - N - 2) + \frac{(N+1)(N+5)}{6}$ . These coefficients satisfy the relations  $\sum_n \alpha_n = \sum_n \beta_n = 0$ ,  $\sum_n \alpha_n^2 = \frac{N(N^2-1)}{12}$ , which leads to (??).  $\square$

We can now finish the proof of Theorem ?? by inserting (??) into (??) to obtain

$$\|U^N(\mathcal{T}) - U^N(\tilde{\mathcal{T}})\| = \frac{a^3 \tilde{k}}{4(1 + \frac{a^2 \tilde{k}^2}{4})^2} \tilde{k}^2 \frac{N(N^2 - 1)}{12} \varepsilon^2 \|U^0\| + \mathcal{O}(\varepsilon^3).$$

$\square$

**2.2. Estimation of the roundoff error due to diagonalization.** The space-time system (??) becomes in the scalar case

$$(B + a^2 I)\mathbf{u} = \mathbf{f},$$

and to diagonalize this system, we need to diagonalize the matrix  $B$ , which will involve unipotent lower triangular Toeplitz matrices.

DEFINITION 2.4. *A unipotent lower triangular Toeplitz matrix of size  $N$  is of the form*

$$(2.12) \quad T(x_1, \dots, x_{N-1}) = \begin{pmatrix} 1 & & & \\ x_1 & \ddots & & \\ \vdots & \ddots & \ddots & \\ x_{N-1} & \dots & x_1 & 1 \end{pmatrix}.$$

The next Lemma gives a closed form eigendecomposition of the time stepping matrix  $B$ , and is proved using the techniques of  $q$ -hypergeometric series (see the book of Gasper and Rahman, *Basic Hypergeometric series* [?]).

LEMMA 2.5 (Eigendecomposition of  $B$ ). *If  $k_n = q^{n-1} k_1$  with  $q \neq 1$ , then  $B$  has the eigendecomposition  $B = VDV^{-1}$ , with  $D = \text{diag}(\frac{4}{k_n^2})$ , and  $V$  and its inverse are unipotent lower triangular Toeplitz matrices given by*

$$(2.13) \quad V = T(p_1, \dots, p_{N-1}), \quad \text{with} \quad p_n := \prod_{j=1}^n \frac{1 + q^j}{1 - q^j},$$

$$(2.14) \quad V^{-1} = T(q_1, \dots, q_{N-1}), \quad \text{with} \quad q_n := q^{-n} \prod_{j=1}^n \frac{1 + q^{-j+2}}{1 - q^{-j}}.$$

*Proof.* The matrix  $B = (C^{-1}B_1)^2$  is diagonalizable if and only if all time steps  $k_n$  are different. The eigenvalues are then  $\frac{4}{k_n^2}$ , and the eigenvectors are those of  $C^{-1}B_1$ . An eigenvector of  $C^{-1}B_1$  is such that  $(B_1 - \frac{2}{k_n}C)X^{(n)} = 0$ , and the matrix  $B_1 - \frac{2}{k_n}C$



is lower bidiagonal, which leads to a recursive formula for the coefficients  $X^{(n)}$  of the eigenvectors,

$$\begin{cases} X_1^{(n)} = X_2^{(n)} = \cdots = X_{n-1}^{(n)} = 0, \\ X_{n+1}^{(n)} = \frac{k_n+k_{n+1}}{k_n-k_{n+1}} X_n^{(n)}, \dots, X_N^{(n)} = \frac{k_n+k_N}{k_n-k_N} X_{N-1}^{(n)}. \end{cases}$$

Since the normalization is arbitrary, we can choose  $X_n^{(n)} = 1$ , which gives

$$X_j^{(n)} = \begin{cases} 0 & \text{for } j < n, \\ \prod_{l=n+1}^j \frac{k_n+k_l}{k_n-k_l} & \text{for } j > n. \end{cases}$$

The matrix of eigenvectors  $V := (X^{(1)}, \dots, X^{(N)})$  is lower triangular and unipotent, i.e. the diagonal elements equal 1. In case of the geometric mesh, it has the particular structure

$$V_{ij} = X_i^{(j)} = \prod_{l=j+1}^i \frac{k_j+k_l}{k_j-k_l} = \prod_{l=j+1}^i \frac{q^j+q^l}{q^j-q^l} = \prod_{l=j+1}^i \frac{1+q^{k-j}}{1-q^{k-j}} = \prod_{l=1}^{i-j} \frac{1+q^l}{1-q^l},$$

which shows that  $V_{ij}$  is a function of  $i-j$  only, and therefore  $V$  is a unipotent Toeplitz matrix. Consider now the inverse of  $V$ . First, it is easy to see that it is also unipotent Toeplitz. To establish (??) is equivalent to prove that

$$(2.15) \quad \text{for } 1 \leq n \leq N-1, \quad \sum_{j=0}^n p_{n-j} q_j = 0, \quad \text{with the convention that } p_0 = q_0 = 1.$$

To show this result, we need to define Heine's  $q$ -hypergeometric series (Heine 1847),

$$(2.16) \quad {}_2\varphi_1(a_1, a_2; b; q; x) := \sum_{n=0}^{\infty} \frac{(a_1; q)_n (a_2; q)_n}{(q; q)_n (b; q)_n} x^n,$$

where we assume that  $b$  is not an integer negative power of  $q$ , and the  $q$ -rising factorial is

$$(a; q)_k := \prod_{i=0}^{k-1} (1 - q^i a), \quad (a; q)_\infty := \prod_{i=0}^{\infty} (1 - a q^i).$$

The Heine's summation formula states that for any two real numbers  $a_1$  and  $a_2$ , and for any  $b$  with  $|b/(a_1 a_2)| < 1$ , we have

$$(2.17) \quad {}_2\varphi_1(a_1, a_2; b; q; b/a_1 a_2) = \frac{(b/a_1; q)_\infty (b/a_2; q)_\infty}{(b; q)_\infty (b/a_1 a_2; q)_\infty}.$$

We now use Heine's summation formula to conclude the proof: let  $N$  be an integer larger than 1; setting  $a_1 = q^{-N}$  and  $a_2 = a$  yields the  $q$ -Chu-Vandermonde formula

$$(2.18) \quad {}_2\varphi_1(q^{-N}, a; b; q; \frac{b}{a} q^N) = \frac{(b/a; q)_N}{(b; q)_N}.$$

Since  $(q^{-N}; q)_n = 0$  as soon as  $n \geq N + 1$ , the series on the left is a finite sum, and we obtain

$$(2.19) \quad \sum_{n=0}^N \frac{(q^{-N}; q)_n (a; q)_n}{(q; q)_n (b; q)_n} \left( \frac{b}{a} q^N \right)^n = \frac{(b/a; q)_N}{(b; q)_N}.$$

This is an equality between rational fractions in  $q$ , which is valid for all  $q$  different from 0, 1, and all  $a \neq 0$  and all  $b$  which are not an integer negative power of  $q$ . Choosing  $a = -q$  and  $b = -q^{-N+2}$ , we have

$$(2.20) \quad (b/a; q)_N = (q^{-N+1}; q)_N = (1 - q^{-N+1}) \cdots (1 - q^{-N+1} q^{N-1}) = 0,$$

and thus the right hand side in (??) vanishes, and we get

$$(2.21) \quad \sum_{n=0}^N \frac{(-q; q)_n (q^{-N}; q)_n}{(q; q)_n (-q^{-N+2}; q)_n} q^n = 0.$$

We express now  $p_n$  in terms of  $q$ -analogues,

$$(2.22) \quad p_n = \prod_{i=1}^n \frac{1 + q^i}{1 - q^i} = \prod_{i=0}^{n-1} \frac{1 + qq^i}{1 - qq^i} = \frac{(-q; q)_n}{(q; q)_n}.$$

Defining  $\tilde{q}_{N-n} := \frac{(q^{-N}; q)_n}{(-q^{-N+2}; q)_n} q^n$  and  $q_{N-n} := \frac{\tilde{q}_{N-n}}{\tilde{q}_0}$ , (??) becomes

$$\sum_{n=0}^N p_n \tilde{q}_{N-n} = \sum_{n=0}^N p_n q_{N-n} = 0.$$

Introducing the definition of  $q_{N-n}$  and performing similar steps as in (??) backwards shows that  $q_n$  is equal to the value in (??), and the proof is complete.  $\square$

In the steps (a) and (c) of the direct time parallel solver (??) based on diagonalization, the condition number of the eigenvector matrix  $S$  has a strong influence on the accuracy of the results, and normalizing the eigenvectors from Lemma ?? with respect to the  $\ell^2$  norm leads to an asymptotically better condition number,

$$(2.23) \quad S := V \tilde{D}, \quad \tilde{D} = \text{diag} \left( \frac{1}{\sqrt{1 + \sum_{i=1}^{N-n} |p_i|^2}} \right).$$

We now study the roundoff error when solving the system  $(B + a^2 I) \mathbf{u} = \mathbf{f}$  numerically using the diagonalization

$$(2.24) \quad S(D + a^2 I) S^{-1} \mathbf{u} = \mathbf{f}.$$

Due to roundoff, we will obtain an approximate solution  $\hat{\mathbf{u}}$ , and the difference between the exact solution  $\mathbf{u}$  and  $\hat{\mathbf{u}}$  is classically related to the condition number of the matrix  $S$ . We first also give such an estimate, but later provide a more accurate one using the structure of the problem at hand.

LEMMA 2.6. Let  $\mathbf{u}$  be the exact solution of  $(B + a^2I)\mathbf{u} = \mathbf{f}$ , and  $\hat{\mathbf{u}}$  be the numerically computed solution using the factored form (??), and let  $\underline{u}$  denote the machine precision. Then for any norm,

$$(2.25) \quad \frac{\|\mathbf{u} - \hat{\mathbf{u}}\|}{\|\mathbf{u}\|} \leq \text{cond}(B) \frac{\|\delta B\|}{\|B\|} \leq (2N + 1)\underline{u} \|B^{-1}\| \| |S| |S^{-1}| \| \|D + aI\|.$$

*Proof.* Using backward error analysis [?], the computed solution satisfies the perturbed systems

$$(S + \delta S_1)\hat{\mathbf{g}} = \mathbf{f}, \quad (D + a^2I + \delta D)\hat{\mathbf{w}} = \hat{\mathbf{g}}, \quad (S^{-1} + \delta S_2)\hat{\mathbf{u}} = \hat{\mathbf{w}},$$

and since  $S$  and  $S^{-1}$  are triangular and  $D$  is diagonal we get (see [?])

$$|\delta S_1| \leq N\underline{u}|S| + \mathcal{O}(\underline{u}^2), \quad |\delta S_2| \leq N\underline{u}|S^{-1}| + \mathcal{O}(\underline{u}^2), \quad |\delta D| \leq \underline{u}|D + aI| + \mathcal{O}(\underline{u}^2).$$

Solving numerically  $(B + a^2I)\mathbf{u} = \mathbf{f}$  using the factored form (??) is equivalent to solving exactly  $(S + \delta S_1)(D + a^2I + \delta D)(S^{-1} + \delta S_2)\hat{\mathbf{u}} = \mathbf{f}$ , which is of the form

$$(B + \delta B)\hat{\mathbf{u}} = \mathbf{f}, \quad |\delta B| \leq (2N + 1)\underline{u}|S| |S^{-1}| |D + aI| + \mathcal{O}(\underline{u}^2).$$

The relative error then satisfies (see [?])

$$(2.26) \quad \frac{\|\mathbf{u} - \hat{\mathbf{u}}\|}{\|\mathbf{u}\|} \leq \text{cond}(B) \frac{\|\delta B\|}{\|B\|} \leq \|B^{-1}\| \|\delta B\|,$$

and inserting  $\|\delta B\|$  from before gives the result in (??).  $\square$

We next provide an asymptotic estimate for the term  $\| |S| |S^{-1}| \|$  on the right in (??) in the case of a geometric time partition using the infinity norm.

LEMMA 2.7 (Asymptotic condition number estimate). For  $q = 1 + \varepsilon$ , we have

$$(2.27) \quad \| |S| |S^{-1}| \|_\infty \sim \frac{2^{2(N-1)}}{(N-1)!} \varepsilon^{-(N-1)},$$

$$(2.28) \quad \text{cond}_\infty(S) \sim \frac{2^{(N-1)} N}{\lfloor \frac{N}{2} \rfloor! \lfloor \frac{N-1}{2} \rfloor!} \varepsilon^{-(N-1)}.$$

*Proof.* Note first that  $|q_n| \sim |p_n| \sim \frac{2^n}{n! \varepsilon^n}$ . We next define  $\gamma_n := \sqrt{1 + \sum_{j=1}^{N-n} |p_j|^2}$  and  $\tilde{d}_n := \frac{1}{\gamma_n}$ , which implies that  $\tilde{D} = \text{diag}(\tilde{d}_n)$ . Then  $\gamma_n \sim |p_{N-n}|$ , and we obtain

$$(2.29) \quad \|S\|_\infty = \max_n \sum_{j=1}^n \frac{|p_{n-j}|}{\gamma_j} \sim \max_n \sum_{j=1}^n \frac{|p_{n-j}|}{|p_{N-j}|} \sim \max_n \sum_{j=1}^n \frac{(N-j)!}{(n-j)!} \left(\frac{\varepsilon}{2}\right)^{N-n} \sim N.$$

By definition  $S^{-1} = \tilde{D}^{-1}V^{-1} = \tilde{D}^{-1}T(q_1, \dots, q_{N-1})$ , that is the line  $n$  of  $T(q_1, \dots, q_{N-1})$  is multiplied by  $\gamma_n$ . Therefore

$$(2.30) \quad \begin{aligned} \|S^{-1}\|_\infty &= \max_n \gamma_n \sum_{j=0}^{n-1} |q_j| \sim \max_n \gamma_n |q_{n-1}| \sim \max_n \gamma_n |p_{n-1}| \\ &\sim \max_n |p_{N-n}| |p_{n-1}| \sim \left(\frac{2}{\varepsilon}\right)^{(N-1)} \max_{1 \leq n \leq N-1} \frac{1}{(n-1)!(N-n)!}. \end{aligned}$$

The last term on the right hand side can be explicitly computed by noting that

$$\max_{1 \leq n \leq N-1} \frac{1}{(n-1)!(N-n)!} = \frac{1}{(N-1)!} \max_{1 \leq n \leq N-1} \binom{N-1}{n-1} = \frac{1}{(N-1)!} \binom{N-1}{\lfloor \frac{N-1}{2} \rfloor},$$

which follows from the Pascal triangle, and thus we get

$$\max_{1 \leq n \leq N-1} \frac{1}{(n-1)!(N-n)!} = \frac{1}{\lfloor \frac{N}{2} \rfloor! \lfloor \frac{N-1}{2} \rfloor!}.$$

Combining (??) and (??) then yields (??). Similarly, we also obtain

$$\begin{aligned} \| |S| |S^{-1}| \|_{\infty} &= \max_i \sum_j (|S| |S^{-1}|)_{ij} = \max_i \sum_{j=1}^i \sum_{k=j}^i |p_{i-k}| |q_{k-j}| \\ &\sim \frac{2^{N-1}}{\varepsilon^{N-1}} \sum_{k=1}^N \frac{1}{(N-k)!(k-1)!} \end{aligned}$$

and explicitly summing the last term on the right,  $\sum_{k=1}^N \frac{1}{(N-k)!(k-1)!} = \frac{2^{N-1}}{(N-1)!}$ , leads to the desired estimate (??).  $\square$

We are now ready to give a precise asymptotic error estimate of the roundoff error that is induced by the diagonalization in the direct time parallel solver (??):

**THEOREM 2.8** (Asymptotic roundoff error estimate). *Let  $\mathbf{u}$  be the exact solution of  $(B + a^2 I)\mathbf{u} = \mathbf{f}$ , and  $\hat{\mathbf{u}}$  be the computed solution from the direct time parallel solver (??) applied to (??), and let  $\underline{u}$  denote the machine precision. Then*

$$(2.31) \quad \frac{\|\mathbf{u} - \hat{\mathbf{u}}\|_{\infty}}{\|\mathbf{u}\|_{\infty}} \lesssim \psi_1\left(\frac{aT}{2N}, N\right) \underline{u} \varepsilon^{-(N-1)},$$

where  $\psi_1(y, N) := \frac{2^{2(N+1)}}{(N-1)!} (1 + 2N(N-1))(1 + y^2)$ .

*Proof.* The form of the matrices involved is very well adapted to estimates in the  $\ell^{\infty}$  norm. We evaluate the various quantities in (??) starting with the norm of  $B^{-1}$ , which we can obtain by computing  $B^{-1} = (B_1^{-1}C)^2$  explicitly and noting that the infinity norm comes from the last line, which gives

$$\|B^{-1}\|_{\infty} = (2k_1)^2 \left( 1 + \frac{2q(q^{N-1} - 1)(q^N - 1)}{(q-1)^2} \right).$$

Now for  $q = 1 + \varepsilon$ , we get by expanding

$$\|B^{-1}\|_{\infty} \sim (2k_1)^2 (1 + 2N(N-1)).$$

We now use that  $D = \text{diag}(\frac{4}{k_i^2})$ , and obtain

$$(2.32) \quad \|B^{-1}\|_{\infty} \|D + aI\|_{\infty} \sim (2k_1)^2 (4/k_1^2 + a^2) (1 + 2N(N-1)) \sim 16(1 + \frac{a^2 k_1^2}{4}) (1 + 2N(N-1)).$$

Inserting (??) into (??) gives

$$\frac{\|\mathbf{u} - \hat{\mathbf{u}}\|_{\infty}}{\|\mathbf{u}\|_{\infty}} \lesssim 16(1 + \frac{a^2 k_1^2}{4}) (1 + 2N(N-1)) \underline{u} \| |S| |S^{-1}| \|_{\infty}.$$

Replacing the last term on the righthand side using (??) leads to

$$(2.33) \quad \frac{\|\mathbf{u} - \hat{\mathbf{u}}\|_\infty}{\|\mathbf{u}\|_\infty} \lesssim \frac{2^{2(N+1)}}{(N-1)!} (1 + 2N(N-1)) \left(1 + \frac{a^2 k_1^2}{4}\right) \underline{u} \varepsilon^{-(N-1)}.$$

Approximating  $k_1$  by  $\tilde{k}$  as  $\varepsilon$  goes to zero finally gives

$$\frac{\|\mathbf{u} - \hat{\mathbf{u}}\|_\infty}{\|\mathbf{u}\|_\infty} \lesssim \frac{2^{2(N+1)}}{(N-1)!} (1 + 2N(N-1)) \left(1 + \left(\frac{aT}{2N}\right)^2\right) \underline{u} \varepsilon^{-(N-1)},$$

which proves the result.  $\square$

REMARK 2.9. *The more usual round off estimates use the condition number of the matrix  $S$  in (??) instead of the norm of  $|S||S^{-1}|$ . Then using (??), the estimate (??) would become*

$$(2.34) \quad \frac{\|\mathbf{u} - \hat{\mathbf{u}}\|_\infty}{\|\mathbf{u}\|_\infty} \lesssim \psi_2\left(\frac{aT}{2N}, N\right) \underline{u} \varepsilon^{-(N-1)},$$

where  $\psi_2(y, N) := \frac{N(1+2N(N-1))2^{N+3}}{\lfloor \frac{N}{2} \rfloor! \lfloor \frac{N-1}{2} \rfloor!} (1 + y^2)$ , which we will see is comparable to our first estimate.

We next present a sharper estimate using the special structure of  $S$  and  $S^{-1}$ .

LEMMA 2.10. *For any  $\mathbf{f}$ , for any diagonal matrix  $\Delta$ , let  $\mathbf{u} = S\Delta S^{-1}\mathbf{f}$ , and  $\hat{\mathbf{u}}$  be the computed value of  $\mathbf{u}$ . Then*

$$(2.35) \quad \|\mathbf{u} - \hat{\mathbf{u}}\|_\infty \lesssim \frac{2^{2(N-1)}}{(N-1)!} \varepsilon^{-(N-1)} \underline{u} \|\Delta\|_\infty \|\mathbf{f}\|_\infty.$$

*Proof.* Standard truncation error estimates as in Theorem ?? show that the approximate value of  $S\Delta S^{-1}\mathbf{f}$  gives an error which can be bounded by

$$\|\overline{S\Delta S^{-1}\mathbf{f}} - S\Delta S^{-1}\mathbf{f}\| \leq \|\mathbf{f}\|_\infty \|\Delta\|_\infty \underline{u} \begin{pmatrix} 1 \\ 1 + |p_1| + |q_1| \\ \vdots \\ |p_{N-1}| + |p_{N-2}|(|q_1| + 1) + \dots \\ + |q_{N-1}| + |q_{N-2}||p_1| + \dots + |q_1| + 1 \end{pmatrix} + \mathcal{O}(\underline{u}^2).$$

Considering the leading term in  $\varepsilon$ , suppose that  $\varepsilon$  and  $N$  are such that the largest coefficient  $p_{N-1}$  satisfies  $|p_{N-1}|\underline{u} \ll 1$ , to obtain

$$\|\overline{S\Delta S^{-1}\mathbf{f}} - S\Delta S^{-1}\mathbf{f}\|_\infty \lesssim \|\mathbf{f}\|_\infty \|\Delta\|_\infty \underline{u} \sum_{n=0}^{N-1} |p_j q_{N-1-j}|.$$

We can estimate the sum using an asymptotic expansion,

$$\sum_{n=0}^{N-1} |p_j q_{N-1-j}| \sim \sum_{n=0}^{N-1} \frac{2^n}{n!} \varepsilon^{-n} \frac{2^{N-1-n}}{(N-1-n)!} \varepsilon^{-(N-1-n)} \sim \frac{2^{2(N-1)}}{(N-1)!} \varepsilon^{-(N-1)},$$

and we obtain

$$(2.36) \quad \frac{\|\overline{S\Delta S^{-1}\mathbf{f}} - S\Delta S^{-1}\mathbf{f}\|_\infty}{\|\mathbf{f}\|_\infty} \lesssim \|\Delta\|_\infty \frac{2^{2(N-1)}}{(N-1)!} \varepsilon^{-(N-1)} \underline{u},$$

which concludes the proof.  $\square$

We can now prove the following sharper estimate for the roundoff error:

**THEOREM 2.11** (Sharper asymptotic roundoff error estimate). *For any  $\mathbf{f}$ , let  $\mathbf{u} = S(D + aI)^{-1}S^{-1}\mathbf{f}$ , and  $\hat{\mathbf{u}}$  be the computed value of  $\mathbf{u}$ . Then*

$$(2.37) \quad \frac{\|\mathbf{u} - \hat{\mathbf{u}}\|_\infty}{\|U^0\|} \lesssim \psi_3\left(\frac{aT}{2N}, N\right) \underline{u} \varepsilon^{-(N-1)},$$

where  $\psi_3(y, N) := \frac{2^{2N-\frac{1}{2}} N}{(N-1)!} \frac{1}{y^{2+1}}$ .

*Proof.* We have  $\|(D + a^2I)^{-1}\|_\infty = \frac{1}{a^2 + \frac{4}{k_N^2}}$ , and replacing  $\Delta$  by  $(D + a^2I)^{-1}$  in (??), we obtain

$$(2.38) \quad \|\mathbf{u} - \hat{\mathbf{u}}\|_\infty \lesssim \frac{2^{2(N-1)}}{(N-1)!} \varepsilon^{-(N-1)} \underline{u} \frac{1}{a^2 + \frac{4}{k_N^2}} \|\mathbf{f}\|_\infty.$$

We need now an estimate of  $\|\mathbf{f}\|_\infty$ , with

$$(2.39) \quad \mathbf{f} = C^{-1}(B_1C^{-1}F_0 + G_0)\mathbf{e}_1, \quad F_0 = \frac{1}{k_1}f + \frac{g}{2}, \quad G_0 = \frac{1}{k_1}g - \frac{a^2}{2}f.$$

We first explicitly compute the inverse of  $C$  and obtain the lower triangular matrix  $C_{ij}^{-1} = 2(-1)^{i-j}$ ,  $i \geq j$ . We can then evaluate the terms in (??) to get

$$(C^{-1}\mathbf{e}_1)_i = 2(-1)^{i-1} \implies (C^{-1}B_1C^{-1}\mathbf{e}_1)_i = 4(-1)^{i-1} \left( \frac{1}{k_1} + 2 \sum_{j=2}^i \frac{1}{k_j} \right),$$

where the sum equals zero for  $i = 1$ . Using that the time steps are geometric,  $k_j = q^{j-1}k_1$ , we define

$$s_i := 1 + 2 \sum_{j=1}^{i-1} \frac{1}{q^j} \text{ for } i \geq 2, \quad s_1 = 1,$$

and obtain  $(C^{-1}B_1C^{-1}\mathbf{e}_1)_i = \frac{4}{k_1}(-1)^{i-1}s_i$ , which we introduce into (??) to get

$$\mathbf{f}_i = (-1)^{i-1} \left( \frac{4}{k_1} F_0 s_i + 2G_0 \right) = (-1)^{i-1} \left( \frac{4}{k_1} s_i \left( \frac{1}{k_1} f + \frac{g}{2} \right) + 2 \left( \frac{1}{k_1} g - \frac{a^2}{2} f \right) \right).$$

Taking the modulus and rearranging terms leads to

$$|\mathbf{f}_i| = \left| \frac{4}{k_1^2} f \left( s_i - \frac{a^2 k_1^2}{4} \right) + \frac{2}{k_1} g (s_i + 1) \right|.$$

Defining  $y_1 := \frac{k_1 a}{2}$ , we obtain

$$|\mathbf{f}_i| = \left| \frac{4}{k_1^2} f (s_i - y_1^2) + \frac{2a}{k_1} \frac{g}{a} (s_i + 1) \right| = \frac{4}{k_1^2} \left| f (s_i - y_1^2) + y_1 \frac{g}{a} (s_i + 1) \right|.$$

For sufficiently small  $k_1$ ,  $y_1$  is smaller than 1, and since  $s_i > 1$  and the sequence  $s_i$  is increasing, we obtain

$$\|\mathbf{f}\|_\infty \leq \frac{4}{k_1^2} (|f|s_N + \frac{|g|}{a}(s_N + 1)) \leq \frac{4}{k_1^2} (s_N + 1)(|f| + \frac{|g|}{a}) \leq \frac{4\sqrt{2}}{k_1^2} (s_N + 1) \|U_0\|.$$

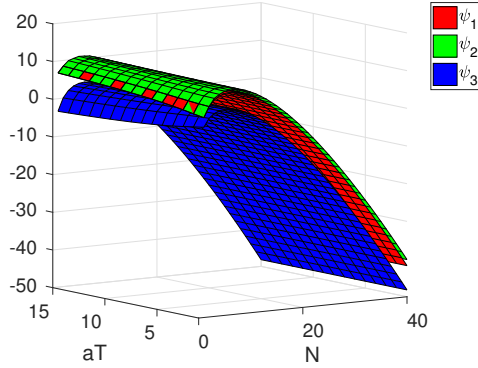


FIG. 2.1. Comparison of the logarithm of the functions  $\psi_j$ ,  $j = 1, 2, 3$

We use now that  $q$  is close to 1 to estimate asymptotically

$$s_N + 1 = 2\left(1 + \sum_{j=1}^{N-1} \frac{1}{q^j}\right) = 2 \sum_{j=0}^{N-1} \frac{1}{q^j} = 2 \frac{1 - \frac{1}{q^N}}{1 - \frac{1}{q}} \lesssim 2N,$$

and therefore

$$\|\mathbf{f}\|_\infty \lesssim \frac{8N\sqrt{2}}{k_1^2} \|U_0\|.$$

This allows us to also estimate  $\|\mathbf{f}\|_\infty$  in (??) asymptotically,

$$\|\mathbf{u} - \hat{\mathbf{u}}\|_\infty \lesssim \frac{2^{2(N-1)}}{(N-1)!} \varepsilon^{-(N-1)} \underline{u} \frac{1}{a^2 + \frac{4}{k_N^2}} \frac{8N\sqrt{2}}{k_1^2} \|U_0\|.$$

We now combine the last two terms asymptotically using that

$$\frac{\frac{4}{k_1^2}}{a^2 + \frac{4}{k_N^2}} \sim \frac{1}{1 + y^2}, \quad y := \frac{aT}{2N},$$

and obtain (??).  $\square$

We show in Figure ?? graphically that  $\psi_1(\frac{aT}{2N}, N)$  and  $\psi_2(\frac{aT}{2N}, N)$  are comparable, while  $\psi_3(\frac{aT}{2N}, N)$  is substantially smaller, and thus gives a much sharper estimate.

**2.3. Optimization of the algorithm parameters.** To start, we perform a numerical experiment for the scalar model problem (??) with  $a = 1$  and initial conditions  $u(0) = 1$ ,  $u'(0) = 0$ . We show in Figure ?? first as a reference the measured discretization error on an equidistant time partition with  $N$  points (called 'error 1', and independent of  $\varepsilon$ ). Next we plot the discretization error due to the geometric time partition, which increases when  $\varepsilon$  is increasing (called 'error 2'), and our theoretical estimate  $\phi\varepsilon^2$  from Theorem ??, which is rather sharp, since it coincides in the figure with the numerically measured values, except for large  $\varepsilon$ . We finally also plot the roundoff error we measure due to the diagonalization procedure, which decreases when  $\varepsilon$  is increasing (called 'error 3'), and our theoretical bound  $\psi_3\varepsilon^{-(N-1)}\underline{u}$  from Theorem ?? . From these plots, we can see that an optimized choice of  $\varepsilon$  would balance these two errors, and for the case on the left with  $T = 5$  and  $N = 10$  (10

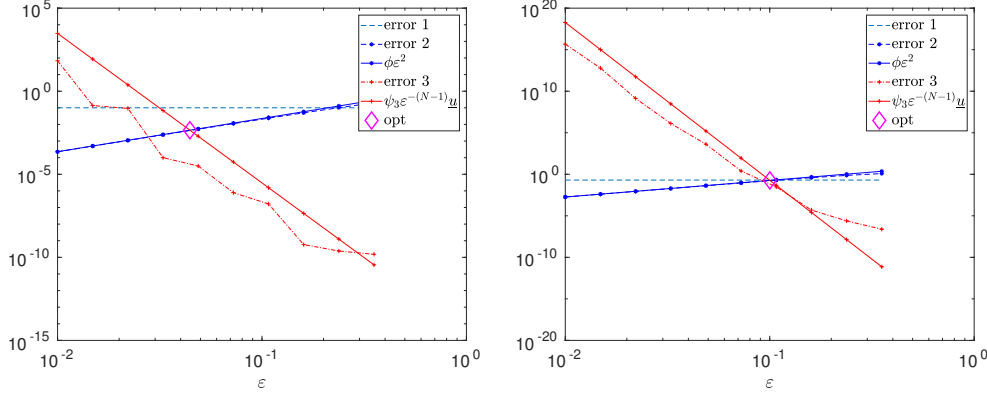


FIG. 2.2. Discretization and parallelization errors, together with our theoretical bounds. Left:  $T = 5$ ,  $a = 1$ ,  $N = 10$ , Right:  $T = 10$ ,  $a = 1$ ,  $N = 20$

processors) it would be  $\varepsilon^* \approx 4.5e - 2$ . In this case, the additional errors due to the time parallelization would remain much smaller than the actual discretization error one would have on an equidistant time grid. For the case on the right in Figure ?? with  $T = 10$  and  $N = 20$  (20 processors), the best choice would be  $\varepsilon^* \approx 1e - 1$ , and now the additional errors due to the parallelization would be of the same order as the actual discretization error one would have on an equidistant time grid.

To determine a formula for the best  $\varepsilon^*$ , we can bound the actual error of the parallel time integrator by adding and subtracting  $u^N(\mathcal{T}_1)$  and also  $u^N(\mathcal{T}_q)$ , with  $q = 1 + \varepsilon$ , and using the triangle inequality, we obtain at time  $T$  an error estimate between the exact solution at time  $T = t_N$  and the last value  $\hat{u}_N$  of the approximate solution computed by diagonalization, namely

$$(2.40) \quad \frac{|u(t_N) - \hat{u}_N|}{\|U^0\|} \leq \underbrace{\frac{|u(t_N) - u^N(\mathcal{T}_1)|}{\|U^0\|}}_{\leq \text{error 1}} + \underbrace{\frac{|u^N(\mathcal{T}_1) - u^N(\mathcal{T}_q)|}{\|U^0\|}}_{\leq \text{error 2}} + \underbrace{\frac{|u^N(\mathcal{T}_q) - \hat{u}_N|}{\|U^0\|}}_{\leq \text{error 3}}.$$

The first term error 1 is the truncation error of the sequential method using equal time steps, see also Figure ?. The second term error 2 is due to the geometric time partition and was estimated asymptotically in Theorem ?? to be  $\phi\varepsilon^2$ . The last term error 3 can be estimated using Theorem ?. Because the second term is decreasing in  $\varepsilon$  and the last term is growing in  $\varepsilon$ , see also Figure ??, we equilibrate them asymptotically and obtain

**THEOREM 2.12** (Optimized geometric time partition). *Suppose the time steps are geometric,  $k_n = q^{n-1}k_1$ , and  $q = 1 + \varepsilon$  with  $\varepsilon$  small. Let  $\underline{u}$  be the machine precision. Fix  $a, T$  and  $N$ . For  $\varepsilon = \varepsilon^*(aT, N)$  with*

$$(2.41) \quad \varepsilon^*(aT, N) = \left( \frac{3 \cdot 2^{2N}}{(N^2 - 1)(N - 1)!} \frac{1 + y^2}{y^3} \underline{u} \right)^{\frac{1}{N+1}}, \quad \text{with } y = \frac{aT}{2N},$$

the error due to time parallelization is asymptotically comparable to the one produced by the geometric time partition.

*Proof.* Equilibration of the error produced by the geometric mesh and the diagonalization means imposing  $\phi(y, N)\varepsilon^2 = \psi_3(y, N)\underline{u}\varepsilon^{-(N-1)}$ , and thus  $\varepsilon^* = \left( \frac{\psi_3}{\phi}(y, N)\underline{u} \right)^{\frac{1}{N+1}}$ ,



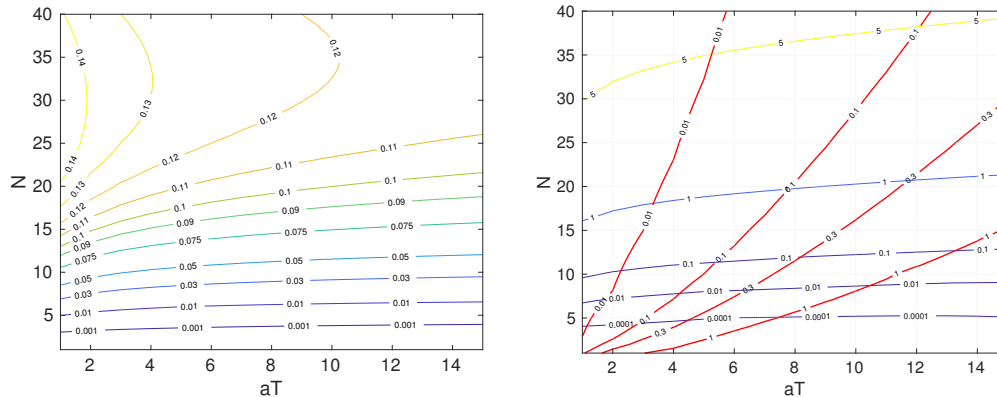


FIG. 2.3. *Left: optimized choice  $\varepsilon^*(aT, N)$  from Theorem ?? . Right: ratio of the additional errors due to parallelization to the truncation error of the fixed step method with this choice of  $\varepsilon^*(aT, N)$  (error 2/error 1), and relative truncation error for a fixed time step method in red (error 1).*

where  $\psi_3$  is defined in Theorem ??, and  $\phi$  is defined in Theorem ?? . Introducing these quantities and simplifying leads to (??).  $\square$

We see in Figure ?? that the theoretically predicted optimized  $\varepsilon^*$  marked by a rhombus is a good estimate of the numerical best parameter. We next show in Figure ?? on the left the optimized value  $\varepsilon^*(aT, N)$  from Theorem ?? as a function of the two arguments  $aT$  and  $N$ . Choosing  $\varepsilon = \varepsilon^*(aT, N)$ , the ratio between the additional errors due to parallelization to the truncation error of the fixed time step method (error 2/error 1) is shown in Figure ?? on the right, together with the relative truncation error for a fixed time step method in red (error 1). We see that one can use approximately 20 processors ( $N = 20$ ) for a reasonably large range of  $aT$  by only increasing the error with the same order one would have had using a sequential integrator on a fixed time mesh, and when using 10 processors, the additional errors due to time parallelization are negligible (about 10% of the errors on an equidistant time grid). When using 40 processors however ( $N = 40$ ), a five fold error has to be expected, due to the parallelization, compared to the sequential time stepping on a fixed time mesh, and this when choosing the best possible value  $\varepsilon = \varepsilon^*(aT, N)$ .

REMARK 2.13. *To obtain an estimate for the best  $\varepsilon$  to chose in the wave equation case, we recall the Fourier transform in space with Fourier variable  $\xi$  which corresponds to our parameter  $a$ . We can thus apply our results from the ODE analysis with  $a^2 = |\xi|^2$ , where  $\xi$  is the dominant frequency in the solution we are trying to calculate. If we have no information about the dominant frequency in the solution, we can also use the upper bound  $\xi_{\max}^2 := \pi^2/h^2$  in 1D ( $h$  the mesh size in space), and  $|\xi_{\max}|^2 := \pi^2/h_1^2 + \pi^2/h_2^2$  ( $h_1$  and  $h_2$  the two mesh sizes in space), since  $\phi\varepsilon^*(aT, N)^2$  is growing in  $aT$ , see Figure ?? on the right. Note that the growth seems to slow down for large values of  $aT$ , so that one can even estimate the value of  $\varepsilon^*(aT, N)$  outside the plotted range of  $aT$ .*

**3. Numerical Experiments.** We now test our theoretical results on the wave equation (??) in one and two spatial dimensions, and also on an industrial test case using the equations of elasticity.

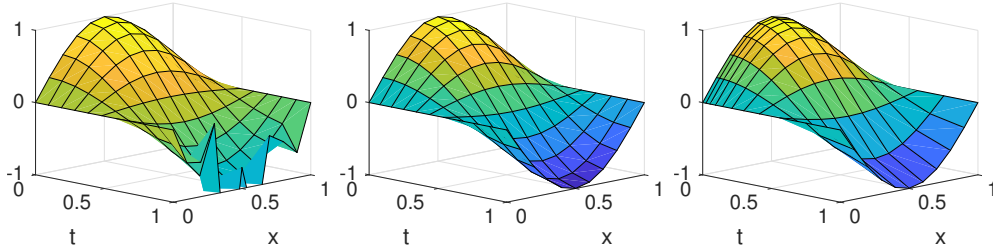


FIG. 3.1. Approximate solutions obtained by the time parallel algorithm using diagonalization. Left:  $\varepsilon = 0.015$ . Middle:  $\varepsilon = \varepsilon^* = 0.05$ . Right:  $\varepsilon = 0.3$ .

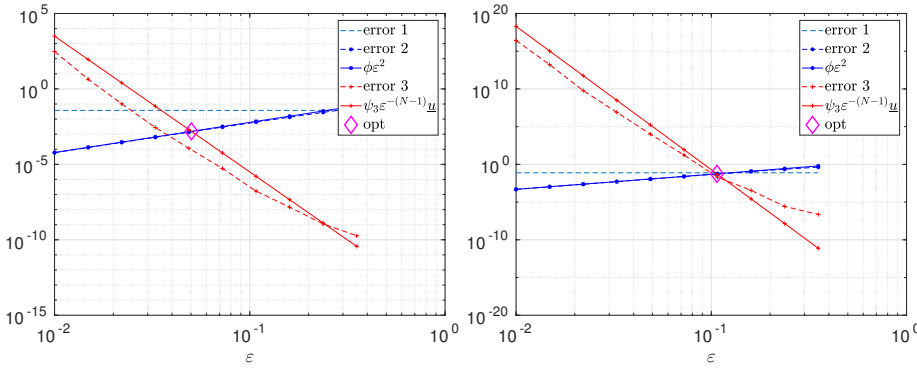


FIG. 3.2. Discretization and parallelization errors in 1d, together with our theoretical bounds for the PDE. Left:  $T = 1$ ,  $N = 10$ . Right:  $T = 2$ ,  $N = 20$ .

**3.1. The wave equation in one dimension.** We solve the wave equation in one dimension on  $[0, 1]$ , with homogeneous Dirichlet boundary conditions and as initial conditions  $u_0(x) = \sin(\pi x)$ ,  $u_1(x) = 0$ . The spatial mesh is  $h = \frac{1}{10}$ , and we use  $N = 10$  time steps on the time interval  $(0, 1)$ . We first show in Figure ?? three numerical solutions obtained for three different geometric time partitions using the diagonalization approach. We clearly see on the left that the  $\varepsilon$  chosen is too small, the solution becomes inaccurate and presents strong oscillations due to the roundoff error introduced by the diagonalization. On the right  $\varepsilon$  is too big, and the solution is less accurate for the second part of the time interval. In the middle, we chose the optimal  $\varepsilon^*$  and obtain an accurate solution, comparable to the one computed sequentially on a fixed step size partition. In Figure ?? we show the corresponding measured discretization and diagonalization errors compared to our theoretical bounds. We see again on the left that for  $T = 1$  using  $N = 10$  (10 processors), using the optimized choice of  $\varepsilon$  leads to a very small error increase compared to the already existing truncation error, as in the ODE case in Figure ?. Using however 20 processors ( $N = 20$ ) on a twice as long time interval  $T = 2$ , the errors due to parallelization are now comparable to the existing truncation error on an equally spaced time grid, and as in the ODE case, one can not use more than about 20 processors for the time parallelization of the wave equation without introducing substantial additional errors due to the parallelization method based on diagonalization.

**3.2. The wave equation in two dimensions.** We now solve the wave equation on the unit square, with homogeneous Dirichlet boundary conditions and as initial

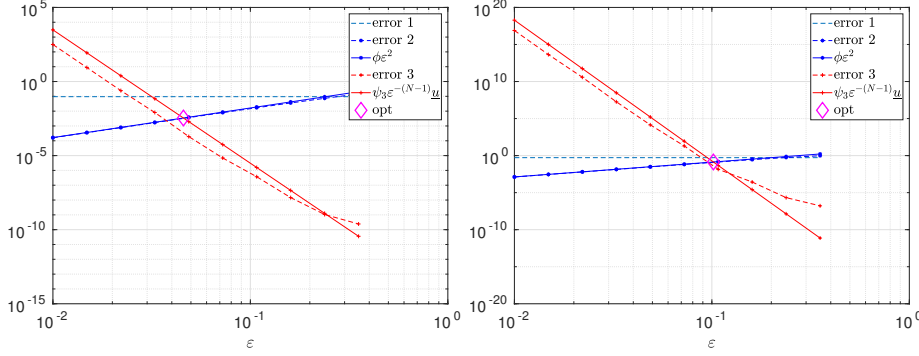


FIG. 3.3. Discretization and parallelization errors in 2d, together with our theoretical bounds for the PDE. Left:  $T = 1$ ,  $N = 10$ . Right:  $T = 2$ ,  $N = 20$ .

conditions  $u_0(x, y) = \sin(\pi x) \sin(\pi y)$ ,  $u_1(x, y) = 0$ , using  $h = \frac{1}{10}$  in space. In Figure ?? we show again the corresponding measured discretization and diagonalization errors compared to our theoretical bounds, and we see that the results are very similar to the one dimensional case.

We also implemented this algorithm on a computer cluster adding to the initial algorithm a time window process in order to compare costs and accuracy for a larger number of time steps, and to truly evaluate parallel performance. We denote by Numwin the number of time windows, where each time window consists of  $N$  time steps. The algorithm now performs 5 steps for each time window, namely

$$\begin{aligned}
 (a) \quad & F = \left( \frac{1}{k_1} u_h^0 + \frac{1}{2} \dot{u}_h^0, \dots, 0 \right) \\
 & G = \left( \frac{1}{k_1} \dot{u}_h^0 + \frac{1}{2} \Delta_h u_h^0, 0, \dots, 0 \right) \\
 (b) \quad & \mathbf{g} = (S_1 \otimes I_x) F + (S_2 \otimes I_x) G, \\
 (c) \quad & \left( \frac{1}{\beta k_n^2} - \Delta_h \right) \mathbf{w}^n = \mathbf{g}^n, \quad 1 \leq n \leq N, \\
 (d) \quad & \mathbf{u} = (S \otimes I_x) \mathbf{w}, \\
 (e) \quad & \dot{\mathbf{u}} = (B_1^{-1} C \otimes I_x) \Delta_h \mathbf{u} + (B_1^{-1} \otimes I_x) G,
 \end{aligned}
 \tag{3.1}$$

where  $S_1 = S^{-1} C^{-1} B_1$  and  $S_2 = S^{-1} C^{-1}$ . Note that step (e) has to be computed in order to initialize  $F$  and  $G$  for the next time window.

All the time matrices are lower triangular matrices and all Kronecker products  $Y = (A \otimes I_x) X$  where  $X = (X_1, X_2, \dots, X_N)$  and  $Y = (Y_1, Y_2, \dots, Y_N)$  can be written as

$$\mathbf{Y} = (A \otimes I_x) \mathbf{X} \iff \begin{cases} Y_1 = A(1,1)X_1 \\ Y_2 = A(2,1)X_1 + A(2,2)X_2 \\ \vdots \\ Y_i = A(i,1)X_1 + A(i,2)X_2 + \dots + A(i,i)X_i \\ \vdots \\ Y_N = A(N,1)X_1 + A(N,2)X_2 + \dots + A(N,N)X_N. \end{cases}$$

For a time window parallel computation with  $N$  processes, each time step  $n$ ,  $1 \leq n \leq N$  is computed by process  $n$ . Steps (a), (b), (c), (d) can be computed in a totally asynchronous manner allowing computing time overlaps, i.e. each process sets up an array where arrays sent from former processes can be stored, then sends the required

$N$	Numwin	Time	Error	Eff
1	128	0.497E+01	5.77E-007	
2	64	0.254E+01	6.13E-007	97.83 %
4	32	0.132E+01	7.71E-007	94.13 %
8	16	0.709E+00	1.71E-006	88.75 %
16	8	0.407E+00	5.15E-005	77.65 %

TABLE 3.1

CPU times for the wave equation in two spatial dimensions. The first row corresponds to the sequential scheme with a fixed time step  $\tilde{k} = \frac{\tilde{T}}{128}$ . We then use time windows depending on  $N$  to get a result over the entire time interval  $(0, \tilde{T})$ . The efficiency  $Eff := \frac{Time(1proc)}{N \times Time(Nproc)}$ .

N	2	4	8	16
CG	0.243E+01	0.125E+01	0.636E+00	0.319E+00
Total	0.254E+01	0.132E+01	0.709E+00	0.407E+00

TABLE 3.2

Detailed CPU times for the solution by CG, compared to the total solution time

data to his successors, computes local data (and other independent computations), then checks data has arrived and then proceeds to step (c) which is independent. Steps (d) and (e) are performed in a similar manner. Once the last processor  $N$  has completed all the 5 steps, it then becomes processor 1 for the next time window, thus saving in communications.

In order to measure the performance, we used in this implementation a  $\mathbb{P}_1$  finite element discretization for step (c), and solved the linear system in space using the conjugate gradient method. Computations were run on a Xeon E5-2680 [Broadwell] @ 2.40 GHz with 28 cores and 512 GB memory, and we used a refined mesh,  $h = \frac{1}{200}$ , with  $\varepsilon = 0.1$ , and simulate the process up to  $\tilde{T} = 1$  using Numwin time windows of length  $T = \tilde{T}/\text{Numwin}$ . We show in Table ?? the measured CPU times. For  $N \leq 16$ , the efficiency of the parallelization by diagonalization is fairly good in this example. In Table ?? we show a comparison where we separate the linear solver time from the rest. The main cost resides in the local linear solver. For  $N > 18$ , the accuracy of the solution deteriorates.

**3.3. Application to a large 3D industrial problem.** We now apply this technique to an industrial problem: we want to compute the response of a carbon/epoxy laminated composite panel to an impact-like loading. This class of material is represented in its linear elastic domain by a transverse isotropic Hooke law. When the fiber direction is aligned with the  $\mathbf{e}_1$  direction, and using the Voigt notation,<sup>1</sup> this Hooke law is given by

$$(3.2) \quad \begin{pmatrix} \varepsilon_{11} \\ \varepsilon_{22} \\ \varepsilon_{33} \\ 2\varepsilon_{23} \\ 2\varepsilon_{13} \\ 2\varepsilon_{12} \end{pmatrix} = \begin{pmatrix} \frac{1}{E_L} & -\frac{\nu_{LT}}{E_L} & -\frac{\nu_{LT}}{E_L} & 0 & 0 & 0 \\ -\frac{\nu_{LT}}{E_L} & \frac{1}{E_T} & -\frac{\nu_{TT}}{E_T} & 0 & 0 & 0 \\ -\frac{\nu_{LT}}{E_L} & -\frac{\nu_{TT}}{E_T} & \frac{1}{E_T} & 0 & 0 & 0 \\ 0 & 0 & 0 & 2\frac{1+\nu_{TT}}{E_T} & 0 & 0 \\ 0 & 0 & 0 & 0 & \frac{1}{G_{LT}} & 0 \\ 0 & 0 & 0 & 0 & 0 & \frac{1}{G_{LT}} \end{pmatrix} \begin{pmatrix} \sigma_{11} \\ \sigma_{22} \\ \sigma_{33} \\ \sigma_{23} \\ \sigma_{13} \\ \sigma_{12} \end{pmatrix}.$$

<sup>1</sup>Voigt notation uses a matrix representation for 4<sup>th</sup> order tensors. It also exploits the symmetries of the 2<sup>nd</sup> order strain and stress tensors (hence the 6 components).

$E_L$	$E_T$	$\nu_{LT}$	$\nu_{TT}$	$G_{LT}$
130.0 GPa	7.7 GPa	0.33	0.4	4750 MPa

TABLE 3.3

Elastic moduli of the T700GC/M21 carbon/epoxy system.

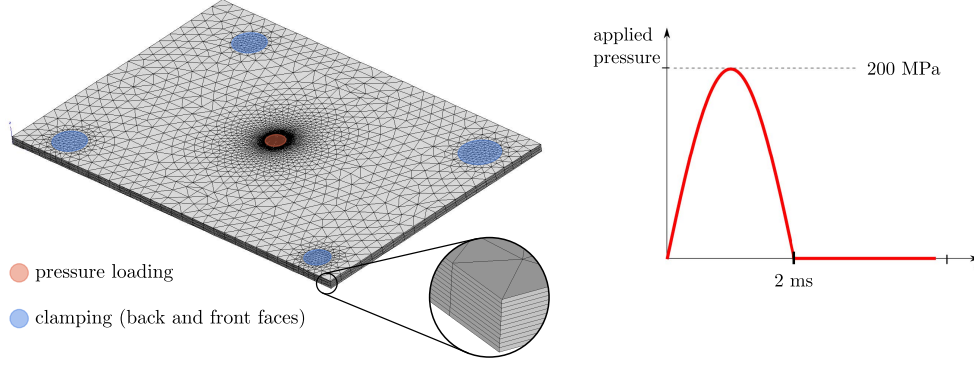


FIG. 3.4. Mesh configuration and loading for the elasticity problem.

Here,  $E_L$  is the longitudinal elastic modulus (in the carbon fiber direction),  $E_T$  is the transverse elastic modulus,  $G_{LT}$  is the elastic shear modulus, and  $\nu_{LT}$  and  $\nu_{TT}$  are the so-called Poisson ratios, and we simulate the elasticity equations,

$$\rho \ddot{\mathbf{u}} = \operatorname{div}(\boldsymbol{\sigma}) + \mathbf{f}, \quad \varepsilon_{ij} = \frac{1}{2} \left( \frac{\partial u_i}{\partial x_j} + \frac{\partial u_j}{\partial x_i} \right).$$

The selected material is a T700GC/M21 carbon/epoxy system used in the aeronautical industry. The corresponding elastic moduli are given in Table ???. The geometry of the problem is taken from the experimental work described in [?]. The tested plate is made of 12 plies with a symmetric stacking sequence. The mesh, illustrated in Figure ??, consists of 152607 degrees of freedom. Dirichlet boundary conditions (represented in blue) are applied on areas representative of the experiment. A homogeneous pressure field is applied at the center of the plate (red circle) and is representative of a small impact. The time is discretized with 2000 time steps over the 10ms simulation range.

The finite element code Zset [?] is used to handle the specific finite element features: mesh generation, material orientation, computation of mass and stiffness matrices, boundary conditions, etc. Zset comes with a Python interface which permits to handle matrices and vectors in a very convenient way through numpy arrays. All the algebraic operations described in equations (??) to (??) are thus performed with the numpy and scipy Python packages. Parallelism is achieved with the mpi4py package, the Python interface to MPI. The script is launched on a 2.4GHz, Xeon E5-2680 processor with 24 cores, but we use only up to  $N = 16$  for our experiments. To reach the 2000 time steps, we thus have to perform  $2000/N$  blocks of parallel solves on so called time windows. There is an evident gain here in using a direct solver, since once the  $N$  sparse operators (see equation (??b)) have been factorized during the first block, their decomposition can be reused for the solutions in the  $2000/N - 1$  remaining blocks. In this implementation, we use the MUMPS solver [?] and its LU decomposition capability. Because of the multiple time windows, we also

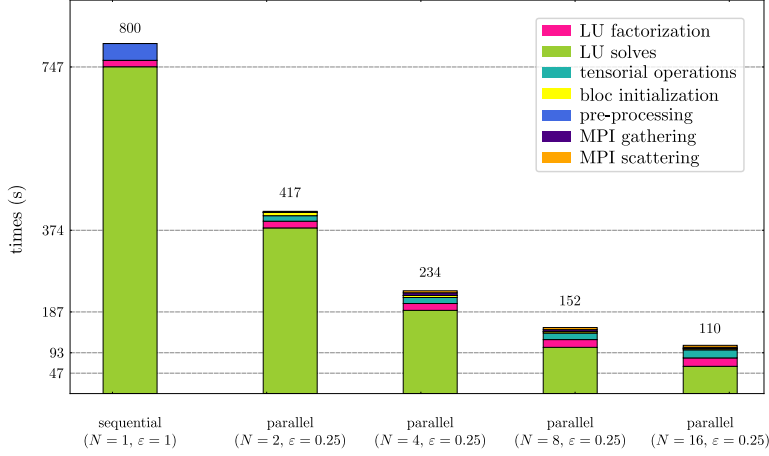


FIG. 3.5. Computing times for the industrial elasticity problem.

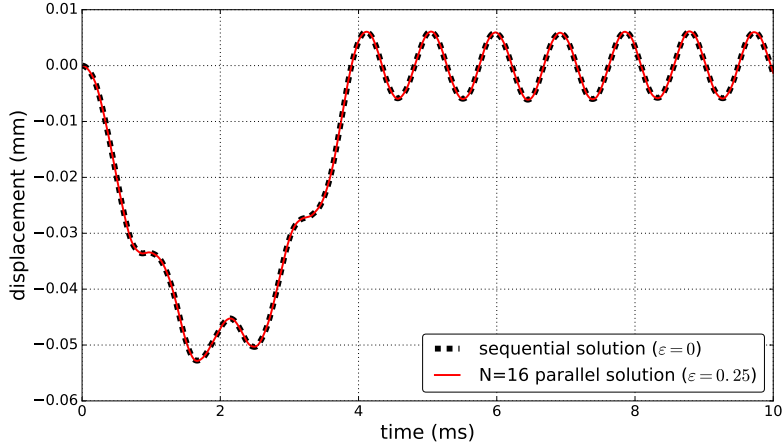


FIG. 3.6. Deflection of the central node on the back face of the plate for the sequential and the parallel solution with  $N = 16$ .

have to properly account for the non-zero initial conditions at the beginning of each block. These operations require additional algebraic operations that we refer to as reinitialization (step  $(e)$  in (??)).

We show in Figure ?? the measured CPU times when parallelizing with different values of  $N$ . The times for the LU factorizations, the LU linear solves by forward and backward substitution, the tensorial operations, the reinitialization, the preprocessing and the MPI communications are shown separately, and we see that the LU linear solves are fully parallelized in time with this diagonalization technique. Figure ?? indeed shows that the corresponding times scale nicely up to  $N = 8$  processors, and one obtains substantial speedup using this method. The overhead due to the different algebraic operations (mainly factorization and tensorial operations) remains about the same from  $N = 2$  to  $N = 16$  but it becomes more significant in the last case (steps  $(b)$  and  $(d)$  in (??)). Figure ?? shows the displacement of the central node on the back face of the plate for the sequential and the parallel solution for  $N = 16$ . No

deviation is noticeable between the two responses, showing that no significant error has been introduced by the parallelization with these parameters.

**4. Conclusions.** We presented and analyzed the time parallelization method by diagonalization for the wave equation. We derived an optimal choice for the geometric stretching of the time grid, balancing carefully truncation and roundoff error. We tested the method numerically for the model wave equation problems in different spatial dimensions, and also on an industrial test case using the elasticity equations. These results show that our theoretical parameters predict well the best choice for the geometric time grid stretching, and substantial speedup is possible when solving wave propagation problems using this technique, and this also in an industrial setting.

#### REFERENCES

- [1] DANIEL BENNEQUIN, MARTIN J. GANDER, AND LAURENCE HALPERN, *A homographic best approximation problem with application to optimized Schwarz waveform relaxation*, *Mathematics of Computation*, 78 (2009), pp. 185–223.
- [2] ANDREW J. CHRISTLIEB, COLIN B. MACDONALD, AND BENJAMIN W. ONG, *Parallel high-order integrators*, *SIAM Journal on Scientific Computing*, 32 (2010), pp. 818–835.
- [3] MATTHEW EMMETT AND MICHAEL L. MINION, *Toward an efficient parallel in time method for partial differential equations*, *Comm. App. Math. and Comp. Sci*, 7 (2012), pp. 105–132.
- [4] ROBERT D. FALGOUT, STEPHANIE FRIEDHOFF, T.V. KOLEV, SCOTT P. MACLACHLAN, AND JACOB B. SCHRODER, *Parallel time integration with multigrid*, *SIAM Journal on Scientific Computing*, 36 (2014), pp. C635–C661.
- [5] CHARBEL FARHAT, JULIEN CORTIAL, CLIMENE DASTILLUNG, AND HENRI BAVESTRELLO, *Time-parallel implicit integrators for the near-real-time prediction of linear structural dynamic responses*, *International Journal for Numerical Methods in Engineering*, 67 (2006), pp. 697–724.
- [6] STEPHANIE FRIEDHOFF, ROBERT D. FALGOUT, T.V. KOLEV, SCOTT P. MACLACHLAN, AND JACOB B. SCHRODER, *A multigrid-in-time algorithm for solving evolution equations in parallel*, in *Sixteenth Copper Mountain Conference on Multigrid Methods*, Copper Mountain, CO, United States, 2013.
- [7] M.J. GANDER, L. HALPERN, J. RYAN, AND T.T.B. TRAN, *A direct solver for time parallelization*, in *Lecture Notes in Computational Science and Engineering*, vol. XXII, Springer, 2015.
- [8] MARTIN J. GANDER, *50 years of time parallel time integration*, in *Multiple Shooting and Time Domain Decomposition Methods*, Springer, 2015, pp. 69–113.
- [9] MARTIN J. GANDER AND STEFAN GÜTTEL, *Paraexp: A parallel integrator for linear initial-value problems*, *SIAM Journal on Scientific Computing*, 35 (2013), pp. C123–C142.
- [10] M. J. GANDER AND E. HAIRER, *Nonlinear convergence analysis for the parareal algorithm*, in *Domain Decomposition Methods in Science and Engineering XVII*, O. B. Widlund and D. E. Keyes, eds., vol. 60, Springer, 2008, pp. 45–56.
- [11] MARTIN J. GANDER AND LAURENCE HALPERN, *Absorbing boundary conditions for the wave equation and parallel computing*, *Math. of Comp.*, 74 (2004), pp. 153–176.
- [12] ———, *Optimized Schwarz waveform relaxation methods for advection reaction diffusion problems*, *SIAM J. Numer. Anal.*, 45 (2007), pp. 666–697.
- [13] MARTIN J. GANDER, LAURENCE HALPERN, AND FRÉDÉRIC NATAF, *Optimal convergence for overlapping and non-overlapping Schwarz waveform relaxation*, in *Eleventh international Conference of Domain Decomposition Methods*, C-H. Lai, P. Bjørstad, M. Cross, and O. Widlund, eds., ddm.org, 1999.
- [14] MARTIN J. GANDER, LAURENCE HALPERN, AND FRÉDÉRIC NATAF, *Optimal Schwarz waveform relaxation for the one dimensional wave equation*, *SIAM Journal of Numerical Analysis*, 41 (2003), pp. 1643–1681.
- [15] MARTIN J. GANDER, FELIX KWOK, AND BANKIM MANDAL, *Dirichlet-Neumann and Neumann-Neumann waveform relaxation algorithms for parabolic problems*, *ETNA*, 45 (2016), pp. 424–456.
- [16] ———, *Dirichlet-Neumann and Neumann-Neumann waveform relaxation for the wave equation*, in *Domain decomposition methods in science and engineering*, DD22, Springer, 2016, pp. pp. 501–509.

- [17] MARTIN J. GANDER, FELIX KWOK, AND HUI ZHANG, *Multigrid interpretations of the parareal algorithm leading to an overlapping variant and MGRIT*, submitted, (2017).
- [18] MARTIN J. GANDER AND MARTIN NEUMÜLLER, *Analysis of a new space-time parallel multigrid algorithm for parabolic problems*, SIAM J. Sci. Comp., 38 (2016), pp. A2173–A2208.
- [19] MARTIN J. GANDER AND MADALINA PETCU, *Analysis of a modified parareal algorithm for second-order ordinary differential equations*, in AIP Conference Proceedings, vol. 936, AIP, 2007, pp. 233–236.
- [20] ———, *Analysis of a Krylov subspace enhanced parareal algorithm for linear problems*, in ESAIM: Proceedings, vol. 25, EDP Sciences, 2008, pp. 114–129.
- [21] MARTIN J. GANDER AND ANDREW M. STUART, *Space time continuous analysis of waveform relaxation for the heat equation*, SIAM J., 19 (1998), pp. 2014–2031.
- [22] MARTIN J. GANDER AND STEFAN VANDEWALLE, *Analysis of the parareal time-parallel time-integration method*, SIAM Journal on Scientific Computing, 29 (2007), pp. 556–578.
- [23] GEORGE GASPER AND MIZAN RAHMAN, *Basic hypergeometric series*, vol. 96, Cambridge university press, 2004.
- [24] ELДАР GILADI AND HERBERT B. KELLER, *Space time domain decomposition for parabolic problems*, Numerische Mathematik, 93 (2002), pp. 279–313.
- [25] GENE H. GOLUB AND CHARLES F. VAN LOAN, *Matrix computations*, Johns Hopkins Studies in the Mathematical Sciences, Johns Hopkins University Press, Baltimore, MD, fourth ed., 2013.
- [26] JAY GOPALAKRISHNAN, JOACHIM SCHÖBERL, AND CHRISTOPH WINTERSTEIGER, *Mapped tent pitching schemes for hyperbolic systems*, arXiv preprint arXiv:1604.01081, (2016).
- [27] GRAHAM HORTON AND STEFAN VANDEWALLE, *A space-time multigrid method for parabolic partial differential equations*, SIAM Journal on Scientific Computing, 16 (1995), pp. 848–864.
- [28] FELIX KWOK, *Neumann–Neumann waveform relaxation for the time-dependent heat equation*, in Domain Decomposition Methods in Science and Engineering XXI, Springer, 2014, pp. 189–198.
- [29] J. L. LIONS, Y. MADAY, AND G. TURINICI, *A parareal in time discretization of PDE’s*, C.R. Acad. Sci. Paris, Serie I, 332 (2001), pp. 661–668.
- [30] C. LUBICH AND A. OSTERMANN, *Multi-grid dynamic iteration for parabolic equations*, BIT, 27 (1987), pp. 216–234.
- [31] YVON MADAY AND EINAR M. RØNQUIST, *Fast tensor product solvers. Part II: Spectral discretization in space and time*, Tech. Report 7-9, Laboratoire Jacques-Louis Lions, 2007.
- [32] ———, *Parallelization in time through tensor-product space-time solvers*, C. R. Math. Acad. Sci. Paris, 346 (2008), pp. 113–118.
- [33] BANKIM MANDAL, *A time-dependent Dirichlet-Neumann method for the heat equation*, in Domain decomposition methods in science and engineering, DD21, Springer, 2014.
- [34] MICHAEL L. MINION, *A hybrid parareal spectral deferred corrections method*, Communications in Applied Mathematics and Computational Science, 5 (2010), pp. 265–301.
- [35] *Mumps: a multifrontal massively parallel sparse direct solver*. <http://mumps-solver.org>.
- [36] NATHAN M. NEWMARK, *A method of computation for structural dynamics*, Journal of the engineering mechanics division, 85 (1959), pp. 67–94.
- [37] JOHANN RANNOU AND JULIET RYAN, *PRF transition statique-dynamique dans les structures composites. rapport technique, année 2. section 1.2*, Tech. Report RT 4/18450 DMSM - février 2012, Onera, 2011.
- [38] ———, *PRF transition statique-dynamique dans les structures composites, rapport technique, année 3, section a.1.1.6*, Tech. Report RT 9/18450 DMSM - 2013, Onera, 2012.
- [39] DANIEL RUPRECHT AND ROLF KRAUSE, *Explicit parallel-in-time integration of a linear acoustic advection system*, Computers & Fluids, 59 (2012), pp. 72–83.
- [40] E. TROUSSET, J. RANNOU, J.-F. MAIRE, AND L. GUILLAUMAT, *Prediction of low-velocity impact damage on composite plates*, in 19th DYMAT Technical Meeting-STRASBOURG, 2011.
- [41] STEFAN VANDEWALLE AND ERIC VAN DE VELDE, *Space-time concurrent multigrid waveform relaxation*, Annals of Numer. Math, 1 (1994), pp. 347–363.
- [42] *Z-set, material and structure analysis suite*. <http://www.zset-software.com>.